

Expanded View Figures

Figure EV1. m6A genes are conserved and functional in planarians.

- A Conservation of the genes encoding the MTC is shown across diversity of organisms. Annotation for *A. thaliana* was obtained from a previous analysis (Růžička et al, 2017).
- B Domain analysis of putative YTH-domain (red block) containing genes.
- C, D The gene expression of planarian MTC and reader-encoding genes, across different cell types and lineages, was extracted from the planarian scRNAseq resource (Plass et al, 2018) (blue to red, low and high expression levels, respectively). The expression of MTC-encoding genes is widespread in different cell types, including in the stem cell compartment (black arrow, indicated in the *mettl3* panel). The expression of reader-encoding genes is not widespread, except for *ythdc-1*, which is expressed across multiple cell types and conditions.
- E Inhibition of m6A genes resulted in lysis of the animals and eventually death. Shown are representative control and *kiaa1429* (RNAi) animals. Scale = 1 mm.
- F Inhibition of m6A genes resulted in defects in food uptake. Shown are animals following feeding with calf liver mixed with a red food color. Control animals show normal food uptake (top) compared with *kiaa1429* (RNAi) animals, which stopped eating. Size measurements were performed on separate animals, which were subjected to the same RNAi treatment. Student's *t*-test; *****P* < 0.0001. Scale = 1 mm.
- G Inhibition of *mettl14* and *ythdc-1* by RNAi has resulted in size reduction. Shown are representative images (left) and measurement of animal sizes following nine RNAi feedings. Significance was calculated using one-way ANOVA followed by Dunnett's multiple comparison test; ****P* < 0.001; **P* < 0.05. Scale = 1 mm.
- H qPCR analysis showed that the gene expression of *mettl3* (top) and *wtap* (bottom) is not downregulated significantly following RNAi, which could likely explain the lack of penetrant phenotypes in these conditions. Error bars indicate the 95% confidence interval. Samples include two technical replicates and at least two biological replicates.
- I Schematic of the design of two non-overlapping gene fragments that were used for synthesis of dsRNA targeting the *kiaa1429* gene. The sequence used for the experiments presented in the manuscript was labeled "original *kiaa1429* clone."
- J dsRNA that was produced using a second cloned fragment of *kiaa1429*, labeled "non-overlapping *kiaa1429* (RNAi)," produced phenotypes that were similar to the phenotypes observed in a non-overlapping clone. This further indicated that the *kiaa1429* (RNAi) phenotype resulted from inhibition of *kiaa1429* gene expression and not because of an off-target effect of the RNAi. Student's *t*-test *****P* < 0.001. Scale = 1 mm.

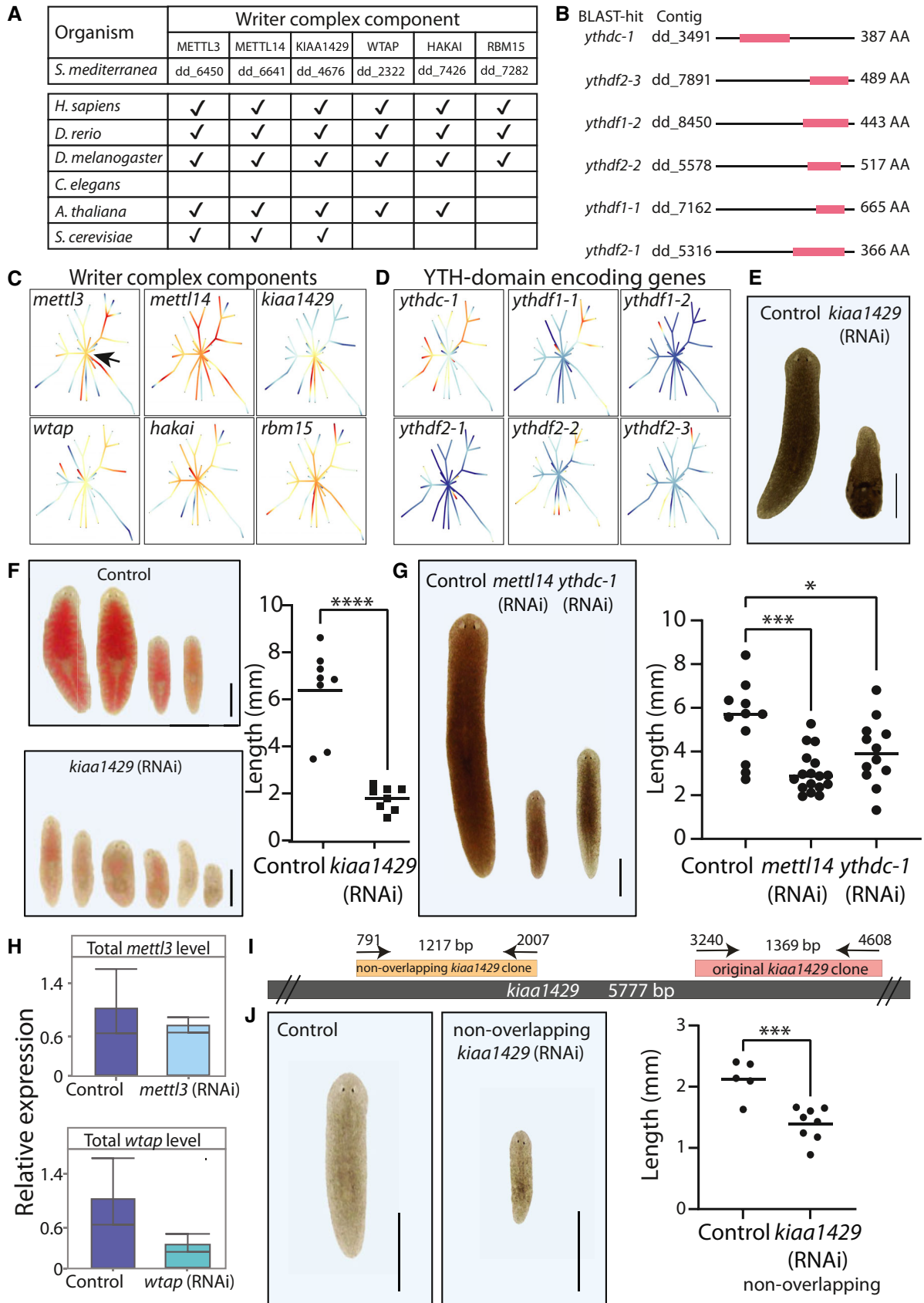


Figure EV1.

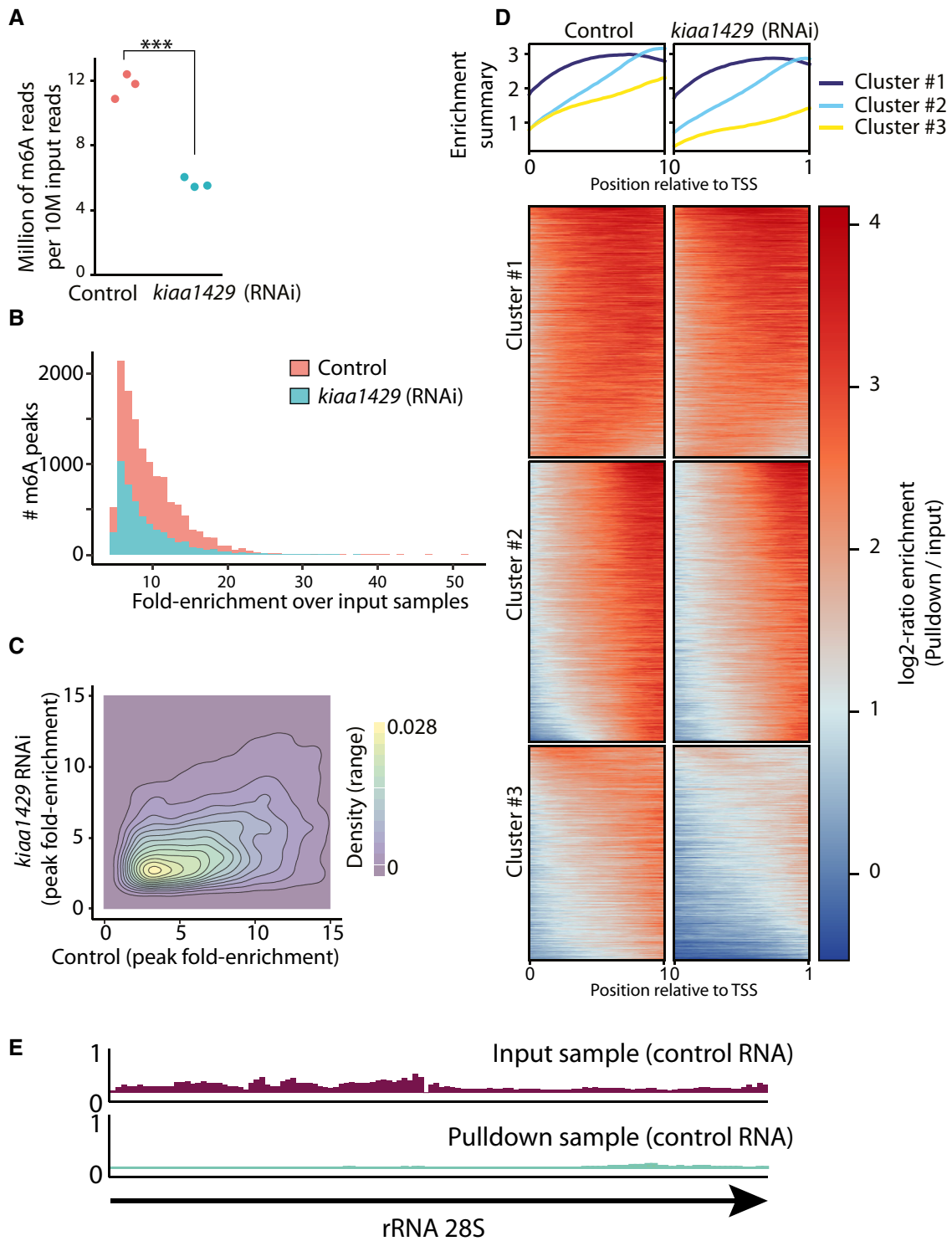


Figure EV2.

Figure EV2. m6A is abundant on planarian mRNA and depleted following *kiaa1429* RNAi.

- A The number of RNAseq reads for each m6A-seq2 pulldown library per 10 M of the corresponding input reads is shown. The number of reads in each pulldown library in the m6A-seq2 protocol correlates with the abundance of m6A (Dierks *et al*, 2021) (red and blue dot, control and *kiaa1429* (RNAi) sample, respectively). ***Student's *t*-test $P < 0.001$.
- B The number of m6A-rich regions (peaks) was larger in control samples and depleted following inhibition of *kiaa1429*. Moreover, the fold-enrichment of the peaks in the control samples over the gene expression observed in the input samples is greater, in comparison to the *kiaa1429* (RNAi) samples.
- C A 2d-density plot showing the correlation between m6A-enriched regions in control and *kiaa1429* (RNAi) animals. The density plot shows that m6a peaks were more highly enriched in the control samples compared to *kiaa1429* (RNAi) samples, demonstrating the depletion of m6A following inhibition of *kiaa1429*.
- D Profile of m6A-enriched regions across genes in control and *kiaa1429* (RNAi) showed enrichment toward the 3'-end. The length of transcripts with detectable m6A-enriched regions was normalized to 1,000 nt. Then, the expression across the transcript was computed by generating bins of gene expression (Materials and Methods) and calculating the log-fold change between the anti-m6A-antibody pulldown library and the input sample. K-means was used to separate three profiles of m6A-enriched regions.
- E Shown is the RPKM normalized expression of the planarian rRNA 28S (block arrow) in the m6A pulldown library and in control. There was no detectable m6A peak on planarian rRNA.

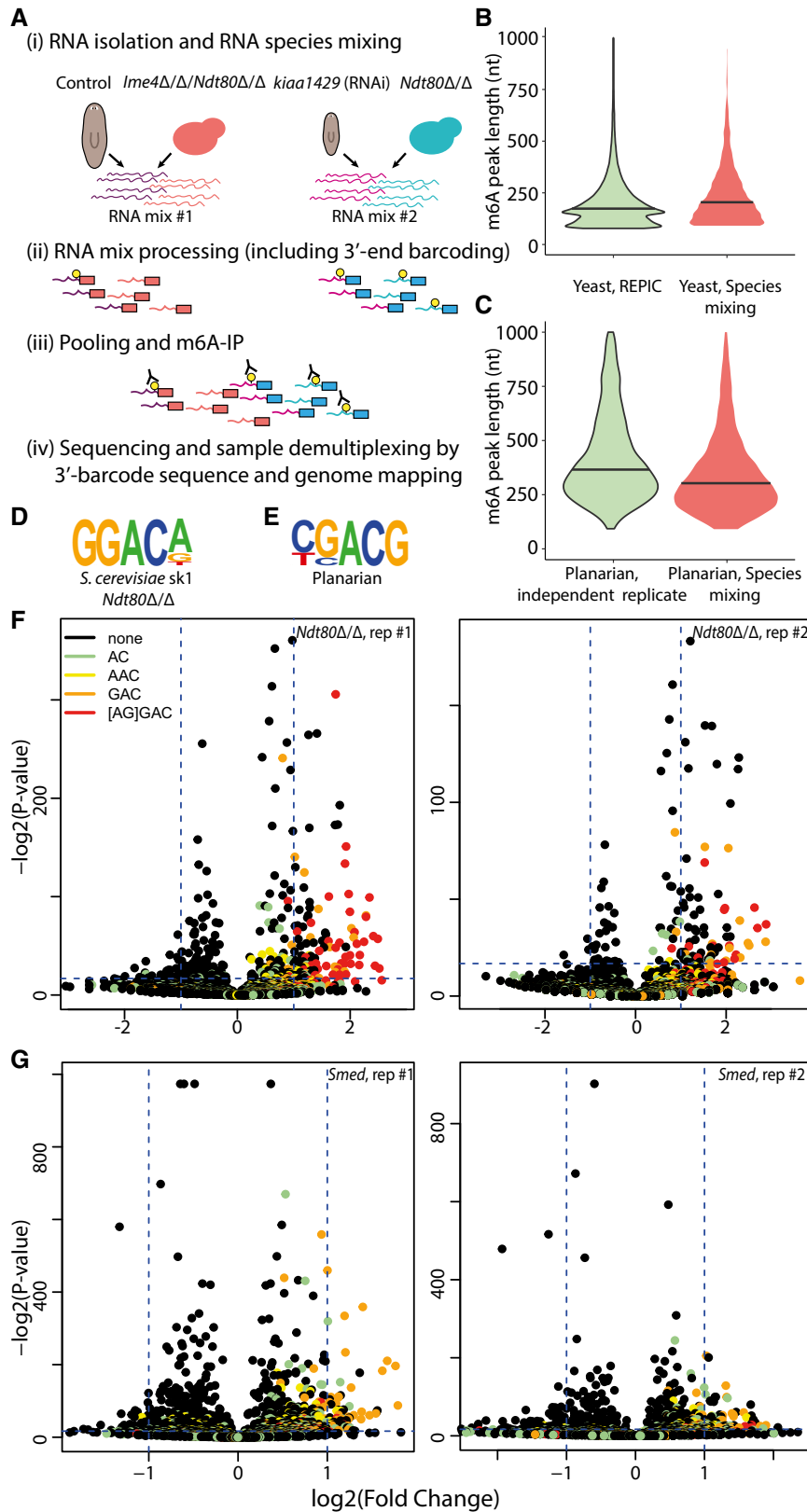


Figure EV3. Analysis of m6A peak length by species mixing experiment.

A RNA was extracted (i) from control or (ii) *kiaa1429* (RNAi) animals in duplicates, with at least 10 animals in each replicate, (iii) from meiosis-blocked *S. cerevisiae* strain with high levels of m6A (*Ndt80Δ/Δ*) (Dierks et al, 2021), and (iv) from *S. cerevisiae* strain devoid of m6A, due to deletion of the methyltransferase (*Ime4Δ/Δ/Ndt80Δ/Δ*). RNA was combined into two pools (Materials and Methods), and was processed according to the m6A-seq2 protocol (Dierks et al, 2021). Following sequencing, reads were associated with the original samples based on their 3'-end barcode (red and blue, representing mix #1 and mix #2, respectively), and then based on their mapping to either the planarian transcriptome or the yeast genome (Materials and Methods).

B Violin plot comparing the length of m6A peaks in yeast from either the REPIC database (Liu et al, 2020c), or from the data collected in this experiment; m6A regions larger than 1,000 bp were excluded from the plot, horizontal line indicates the median length.

C Comparison of planarian m6A peaks in our initial m6A-seq2 experiment, and in the m6A-seq2 profiling in the species RNA mixing experiment. Shown are peaks shorter than 1,000 bp. To avoid comparison of lowly enriched peaks, shown are peaks with fold-enrichments that are larger than the median fold-enrichment.

D, E Shown is the most frequent sequence motif detected in our mixed m6A-seq2 experiment (Materials and Methods), as detected by HOMER (Heinz et al, 2010) for yeast (D) and planarian (E).

F, G Shown are the fold change and associated P-values for each k-mer. DRACH-like k-mers are colored as in the figure legend. Data is shown for yeast (F; panels represent two biological replicates) and planarian (G; panels represent two biological replicates).

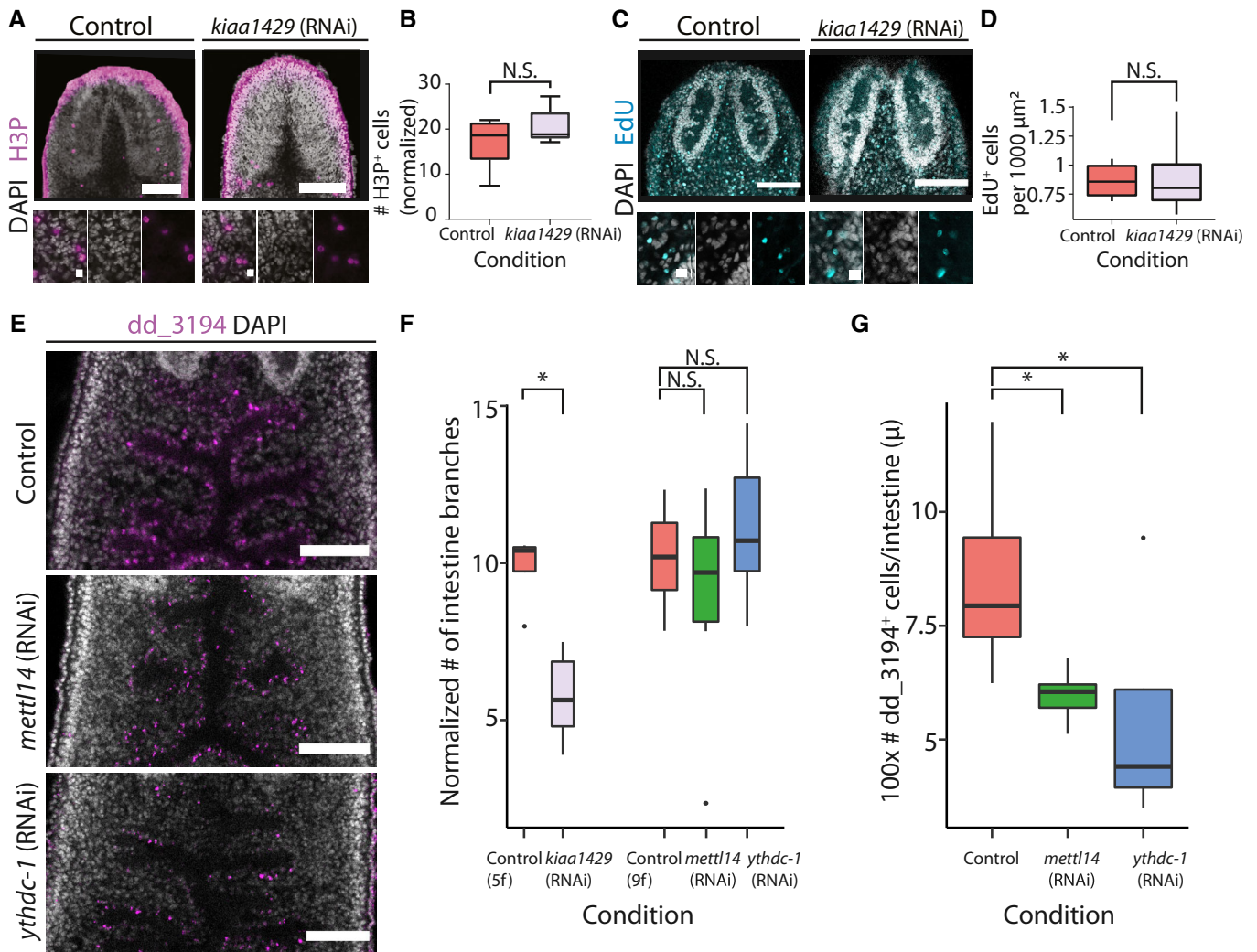


Figure EV4. Reduction in intestinal cells following inhibition of m6A genes.

A, B Shown is H3P labeling using an anti-H3P-antibody in *kiaa1429* (RNAi) and in control animals (scale = 100 and 10 μm, top and bottom panels, respectively; top panels show a maximal intensity projection of the H3P and DAPI signal; [Materials and Methods](#)). (B) The number of H3P⁺ cells was counted in a region anterior to the pharynx and posterior to the brain, in a z-stack and was normalized to the area of the counting ([Materials and Methods](#)). There was an insignificant difference in the number of H3P⁺ cells between the conditions (Student's *t*-test; *n* = 6 biological replicates). Boxes represent the IQR, whiskers represent the 1.5 × IQR, and central band represents the median.

C, D Shown are confocal images of *kiaa1429* (RNAi) and control animals, which were soaked in F-ara-EdU for 16 h (scale = 100 and 10 μm, top and bottom panels; [Materials and Methods](#)). (D) The number of F-ara-EdU⁺ cells was counted in a region anterior of the pharynx and posterior to the brain and was normalized to the rectangle size ([Materials and Methods](#)). There was an insignificant difference in the number of F-ara-EdU⁺ cells between the tested conditions (Student's *t*-test; *n* = 5 biological replicates). Boxes represent the IQR, whiskers represent the 1.5 × IQR, and central band represents the median.

E–G The effect of inhibition of m6A pathway-encoding genes on the intestine integrity and cells was examined by FISH. (E, F) Inhibition of *mettl14* (RNAi) or *ythdc-1* (RNAi) by 9 dsRNA feedings did not result in significant differences in the morphology of the intestine, as estimated by counting the number of intestine branches in confocal images ([Materials and Methods](#)). A significant difference in the number of intestine branches was observed following *kiaa1429* (RNAi) following five RNAi feedings compared to its control. Scale = 100 μm. (E, G) A significant reduction in the number of intestine cells labeled by dd_3194 was found following either *mettl14* (RNAi) or *ythdc-1* (RNAi) (two-sided *t*-test controlled by Bonferroni's correction). The dd_3194⁺ cells were counted in confocal images and the counting was normalized to the length of the intestine branches ([Materials and Methods](#)). **P* < 0.05.

Figure EV5. Analysis of *kiaa1429* (RNAi) phenotypes by scRNAseq.

- A–D Quality measurements of scRNAseq libraries prepared from control and *kiaa1429* (RNAi) cells. The quality of the libraries produced from both conditions was assessed using the Seurat package (Stuart *et al*, 2019). The number of expressed genes (A); unique molecular tags (B); non-coding gene expression (C); and the correlation between the number of expressed genes and the unique molecular tags were highly similar between the libraries (D). This indicated that the quality of libraries was comparable.
- E Expression levels of canonical neoblast markers were highly similar in control and *kiaa1429* (RNAi).
- F The polyadenylated transcript expression of *h2b* and *h3* was much higher in *kiaa1429* (RNAi) animals compared to controls. The expression was detectable in neoblasts (bottom), and to a much lesser degree in the entire cell population (top), which includes neoblasts as well.
- G, H UMAP representation of neoblasts (color dots, left panel), and their identity (right panel). Neoblast identity was assigned based on expression of previously published gene expression markers (Fincher *et al*, 2018). Most neoblast clusters were not affected by the RNAi, yet several lineages (right, asterisk) were differentially represented following *kiaa1429* (RNAi).
- I Expression of neoblast (*smedwi-1*) and specialized intestine neoblast gene expression markers was overlaid on UMAP plots of the intestine lineage (cells represented by dots; gray and purple, low to high ranked expression).
- J–L Comparison of gene expression between several cell clusters. Importantly, pharynx cells are post-mitotic, and therefore show minimal *smedwi-1* expression (J). Post-mitotic cells express *xbp-1*, which was previously shown to be expressed in differentiating and differentiated cells (Raz *et al*, 2021) (K). *SMAD6/7–2* is expressed in the *kiaa1429* (RNAi) specific-cluster and in neural cells (L).
- M Highly expressed genes in the *kiaa1429* (RNAi)-specific cluster compared to control are shown in UMAP plots. Contig dd_1620 is highly expressed in the *kiaa1429* (RNAi)-specific cluster. The genes *SMAD6/7–2* and *protocadherin-like* (dd_15376, gene model SMESG000067388) are expressed in the *kiaa1429* (RNAi)-specific cluster (black arrowhead); both genes are also expressed in cells of the neural clusters (e.g., cluster 2).

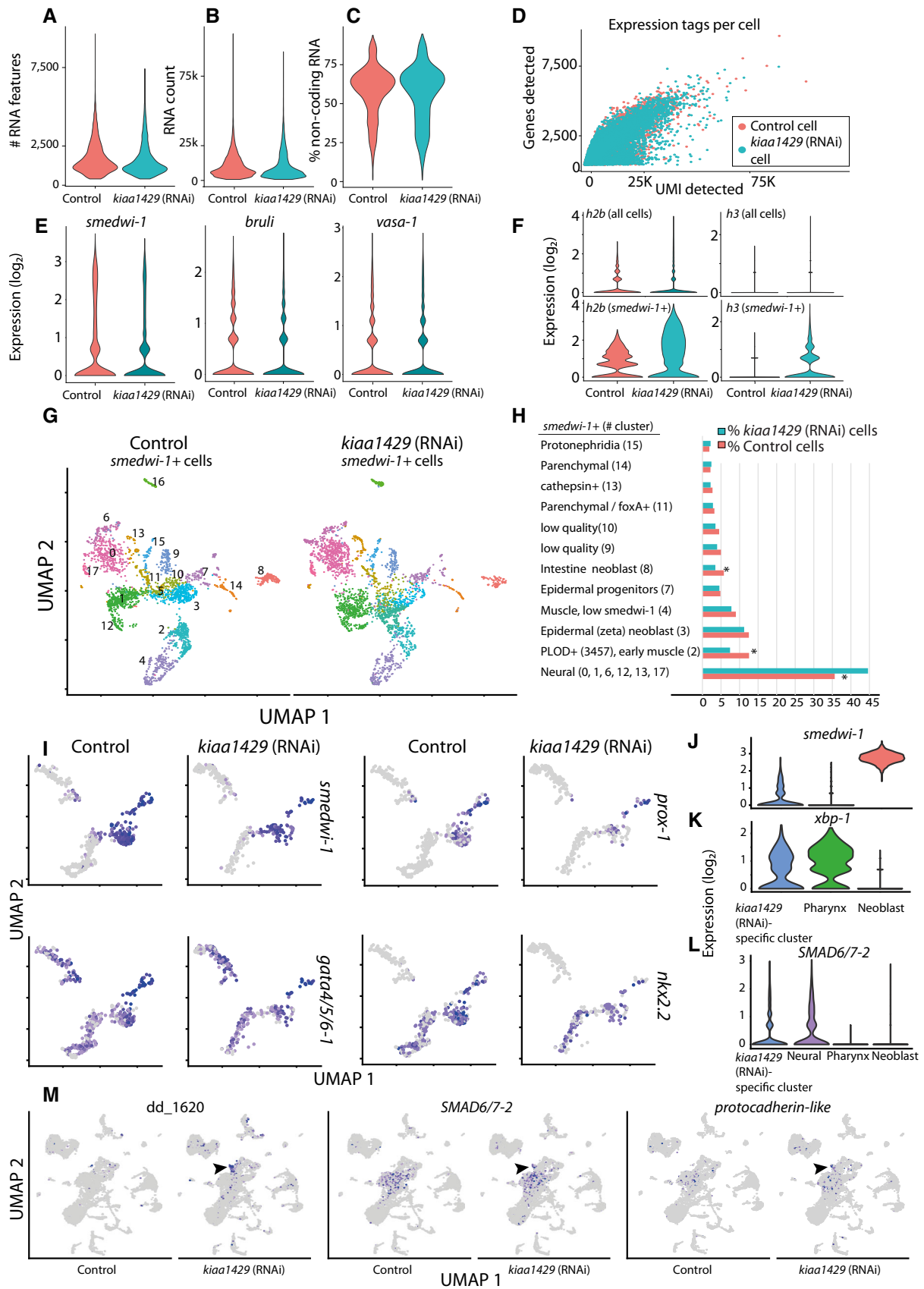


Figure EV5.